Fault-Line Identification of HVDC Transmission Lines by Frequency-Spectrum Correlation Based on Capacitive Coupling and Magnetic Field Sensing

Ke Zhu, W. K. Lee, and Philip W. T. Pong

Department of Electrical and Electronic Engineering, The University of Hong Kong, Hong Kong

The protection system of high-voltage direct-current (HVDC) system must detect, identify, and isolate the fault quickly to keep the system stable by only isolating the components that are under fault, while leaving the rest of the network in operation. However, the criteria of under-voltage and voltage-derivative protection systems may fail because there also arises a large voltage drop/variation on the healthy transmission line due to the electromagnetic coupling among HVDC transmission lines incurred by the sharp transient current in the faulty line. Thus, a fault-line identification technique of HVDC transmission lines by frequency-spectrum correlation was proposed in this paper, which is based on evaluating the similarity degree of frequency spectrum between the voltage of a line and the current of another. This technique was implemented and validated by simulation on a ±500 kV HVDC transmission system. The simulation model was integrated with a capacitive-coupling and magnetic-field-sensing-assisted platform comprised two paralleled induction bars, and an array of magnetic sensors to measure voltage and current. This identification technique can enhance the reliability of HVDC system by avoiding the unnecessary outages due to accidental shutdown of healthy lines, fostering the HVDC system development.

Index Terms— **Capacitive coupling, electromagnetic coupling, fault line, high-voltage direct-current (HVDC), magnetic sensing.**

I. Introduction

THE high-voltage direct-current (HVDC) system, as a critical enabler in the future energy system based on renewables, is reshaping the structure of the traditional power system [1]–[3]. The HVDC is also efficient and economical to interconnect faraway power centers which may be under asynchronous frequency. As such, HVDC is rising in popularity around the globe, and it forms an important component of the latest development of power system [4], [5].

The purpose of the HVDC protection system is to remove the main in-service circuit equipment at abnormal operation promptly (e.g., short-circuit fault) that might cause damage or interfere the neighboring system [6]. The most commonly used protection system for HVDC transmission lines is under-voltage and voltage-derivative protection, as displayed in Fig. 1 [7]. When a fault (e.g., line-to-ground short-circuit fault) occurs on an HVDC transmission line, the faulty line voltage (U_{DL}) drops to a very low threshold ($|U_{\mathrm{DL}}| < \Delta_2$) at a fast rate ($|dU/dt| > \Delta_1$), tripping the corresponding relays [8]. However, the criteria of the protection system may fail because there also arises a large voltage drop/variation on the healthy transmission line due to the electromagnetic coupling between HVDC transmission lines incurred by the sharp transient current in the faulty one. As such, the healthy line could be mistakenly identified and isolated, resulting in unnecessary disruption and delaying system restoring time.

In this paper, the primary method to tackle the mentioned problem is voltage de-coupling method [8]. In this method,

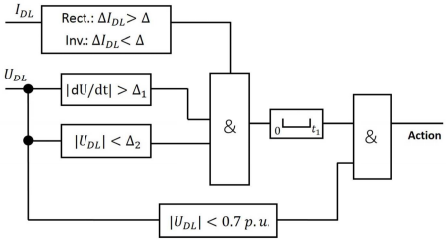

Fig. 1. Logic diagram of under-voltage and voltage-derivative protection systems.

the voltage of a line is supposed to be coupling with another by a coefficient ($0 < k < 1$). Under transient status, the measured voltage can be de-coupled into several independent module components. For example, the independent module coefficients for a single-circuit HVDC transmission line are

$$\begin{bmatrix} \Delta U_e \\ \Delta U_f \end{bmatrix} = \begin{bmatrix} 1 & 1 \\ 1 & -1 \end{bmatrix} \begin{bmatrix} \Delta U_p \\ \Delta U_n \end{bmatrix} \tag{1}$$

where ΔU_e is a ground mode component, ΔU_f is the line mode component, and ΔU_p and ΔU_n are the measured voltage variations on HVDC transmission lines of positive and negative polarities, respectively. For a phase-to-ground fault on the positive polarity ($\Delta U_p = \Delta U_k$ and $U_n = k\Delta U_k$, where ΔU_k is the absolute voltage variation on the faulty line), or on the negative polarity ($\Delta U_n = -\Delta U_k$ and $U_p = -k\Delta U_k$), the polarity of independent module components can be summarized in Table I. It can be seen that the faulty line can be discriminated from different combinations of module-component polarities. However, the accuracy of this method can be affected by two issues [9]. First, since the coupling coefficient (k) is unknown, it is not easy to set an absolute threshold to differentiate the voltage variation occurred between the normal and fault conditions by just

Manuscript received March 15, 2018; accepted April 20, 2018. Date of publication May 15, 2018; date of current version October 17, 2018. Corresponding author: P. W. T. Pong (e-mail: ppong@eee.hku.hk).

Color versions of one or more of the figures in this paper are available online at http://ieeexplore.ieee.org.

Digital Object Identifier 10.1109/TMAG.2018.2830803

TABLE I
MODULE COMPONENT BY DE-COUPLING METHOD

Fault	ΔU_e	Polarity	ΔU_f	Polarity
P	$(1+k)U_k$	+	$(1-k)U_k$	+
N	$-(1+k)U_k$	-	$(1-k)U_k$	+

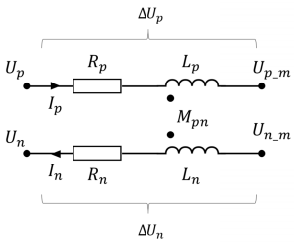

Fig. 2. Equivalent circuit for a single-circuit HVDC transmission line.

investigating the polarity of the independent module component in Table I. Second, this change might not be the same as the one of the HVDC transmission lines induced by electromagnetic coupling because the voltage variation is measured within the substation, but some HVDC transmission systems are connected with dc filters and some frequency components are removed [10], [11]. Therefore, it is necessary to develop a more reliable fault-line identification technique.

In this paper, a fault-line identification technique based on the frequency-spectrum correlation is developed in order to distinguish the healthy HVDC transmission line from the faulted one. In Section II, the working principle of the technique is explained by taking the equivalent circuit of a single-circuit HVDC system as an example to model the voltage and current relation between HVDC transmission lines. Then, this technique was implemented on a ±500 kV single-circuit HVDC system which was established in PSCAD/EMTDC [12] based on capacitive coupling and magnetic field sensing in Section III. The discussion and conclusion are drawn in Section IV.

II. WORKING PRINCIPLE

A. Electromagnetic Coupling

In order to study the voltage and current relation between HVDC transmission lines, an equivalent circuit is established in Fig. 2 by taking a single-circuit HVDC transmission line as an example. The current and voltage of the transmission lines are drawn for the positive (U_p, I_p) and negative (U_n, I_n) polarities, respectively. As such, the voltage of one transmission line can be correlated with the current of the other line as (taking the voltage of negative polarity as an example) [8]

$$U_{nm}(t_2) = U_n\left(t_2) - (I_n(t_2) \times R_n + L_n\frac{dI_n}{dt} - M_{pn}\frac{dI_p}{dt}\right) \quad (2)$$

$$\frac{dI_n}{dt} = \frac{I_n\,(t_2) - I_n(t_1)}{t_2 - t_1}, \quad \frac{dI_p}{dt} = \frac{I_p\,(t_2) - I_p(t_1)}{t_2 - t_1} \quad (3)$$

where U_n (U_{nm}) is the voltage measured at the substation (on a point of transmission line), I_n (I_p) is the line current for the negative (positive) pole, R_n (L_n) is the line resistance (self-inductance), M_{pn} is their mutual inductance, and $(dI_n/dt)(dI_p/dt)$ is the negative (positive) current change rate within a time from t_1 to t_2. Based on (2) and (3), the voltage characteristic under the normal and faulty status can be illustrated as follows.

1) *Normal Status:* The current changing rate (dI_n/dt, dI_p/dt) is almost 0 in the normal status since the current is stable apart from minor harmonics. In this status, (2) can be simplified as

$$U_{nm}(t_2) = U_n(t_2) - (I_n(t_2) \times R_n) \quad (4)$$

which describes the voltage drop across the line due to the line resistor.

2) *Transient Status:* There is a large current variation (dI_p/dt) when a grounding fault occurs on the positive transmission line. A large voltage variation is induced through the electromagnetic coupling by mutual inductance (M_{pn}) on the healthy transmission line. Therefore, the under-voltage and voltage-derivative protection systems can be tripped even though there is no fault on this healthy transmission line.

B. Frequency-Spectrum Correlation

By taking the Fourier transform of (2), the equation becomes

$$F(U_{n_m}(t_2)) = F(U_n(t_2)) - \left(R_n F(I_n(t_2)) \times + L_n F\left(\frac{dI_n}{dt}\right) - M_{pn} F\left(\frac{dI_p}{dt}\right)\right) \quad (5)$$

where $F(\cdot)$ is the Fourier Transform of the included function [13]. By looking into (5), the frequency spectrum of voltage ($F(U_{n_m}(t_2))$) must exhibit a similar pattern as the one of the varied current [$F(dI_p/dt)$] when this voltage variation is induced by the current change. Therefore, the similarity degree of frequency spectrum between voltage of a line and current of another can be used to determine whether the voltage variation is incurred by electromagnetic coupling or fault, and thus avoiding false operation of protection system. In order to evaluate the similarity of two frequency spectrums, the correlation coefficient [14], [15] is adopted to attain the strength and the direction of a linear relationship between the two variables. It is mathematically expressed as

$$r(f,g) = \frac{\sum_{i=1}^{n}(f(i) - \bar{f})(g(i) - \bar{g})}{\sqrt{\sum_{i=1}^{n} f^2(i)}\sum_{i=1}^{n} g^2(i)} \quad (6)$$

where $f(i)$ and $g(i)$ are the intensity of frequency spectrum at frequency i. The value of correlation coefficient is between -1 and 1, and $+1$ indicates a perfect positive fit, 0 indicates no correlation, and -1 indicates a perfect negative fit.

III. SIMULATION VALIDATION

A. Technique Validation

In order to validate the proposed technique, a ±500 kV HVDC transmission system connecting two ac system [12] was established in PSCAD/EMTDC, as displayed in Fig. 3(a).

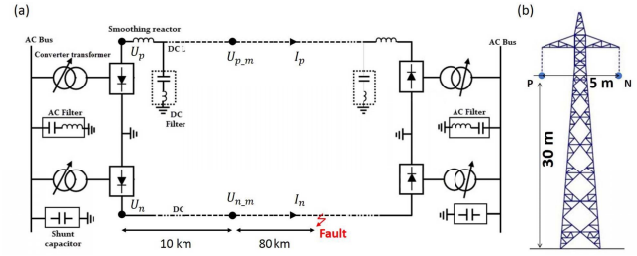

Fig. 3. Simulation model of a ±500 kV single-circuit HVDC transmission system. (a) HVDC system interconnecting two ac systems: base 100 MVA (three phase), voltage (L–L, rms) for systems 1 and 2 are 362.25 and 241.5 kV at 50 Hz, respectively. (b) Height of HVDC transmission lines is 30 m with a 5 m spacing distance.

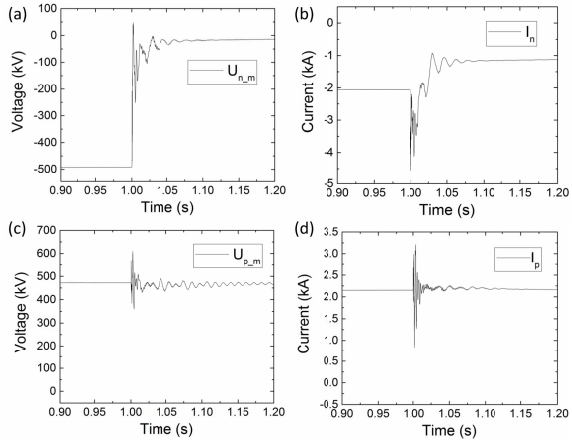

Fig. 4. Real-time voltage and current record. (a) Voltage measured at sensing point of the negative polarity. (b) Current measured for the negative polarity. (c) Voltage measured at sensing point of the positive polarity. (d) Current measured for the positive polarity.

The HVDC system consists of rectifier and inverter station and dc transmission lines. The total length of HVDC transmission lines is 110 km, and the spatial layout of line conductors is displayed in Fig. 3(b). The voltage and current measurement points are 10 km away from the rectifier side, and a line-to-ground fault is simulated 90 km from the substation at 1 s at the negative polarity in the steady status of system operation.

The real-time record of voltage and current for the positive and negative polarities is displayed in Fig. 4. Due to a phase-to-ground short circuit at the negative polarity, its voltage at the measurement point drops to almost 0 with a fluctuation [Fig. 4(a)], and the same occurs for the line current [Fig. 4(b)]. Though there is no fault occurred on the positive pole of HVDC transmission line, its voltage also fluctuates with a large amplitude [Fig. 4(c)] due to electromagnetic coupling with the negative pole. The corresponding fluctuation of current on the negative pole can be seen in Fig. 4(d). Under this condition, the under-voltage and voltage-derivative protection may be inadvertently triggered by the voltage variation on this healthy line. The frequency spectrum was analyzed for the voltage and current with a 0.005 s time window (from 1.000 to 1.005 s) after fault, as displayed in Fig. 5. A high similarity can be observed for the frequency spectrum between the voltage of positive polarity and the current of negative

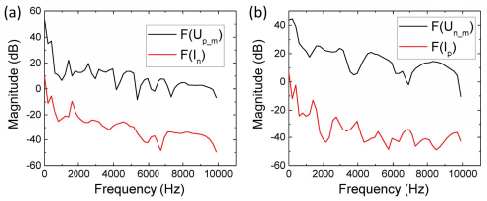

Fig. 5. Frequency spectrum with a 0.005 s time window after fault occurred at 1 s. (a) Frequency spectrum for the voltage of positive polarity and the current of negative polarity. (b) Frequency spectrum for the voltage of negative polarity and the current of positive polarity.

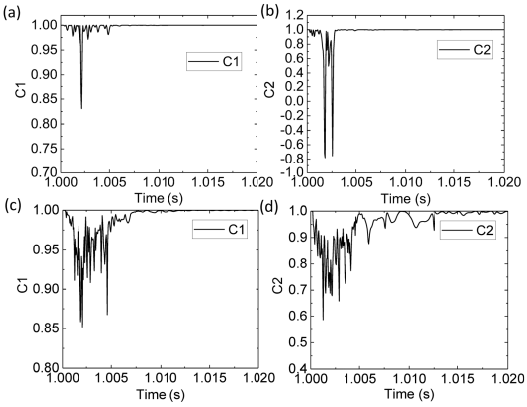

Fig. 6. Correlation coefficient. (a) C_1 for a 0.0005 s sampling time. (b) C_2 for a 0.0005 s sampling time. (c) C_1 for a 0.002 s sampling time. (d) C_2 for a 0.002 s sampling time.

polarity [Fig. 5(a)] but not in the frequency spectrum between the voltage of negative polarity and the current of positive polarity [Fig. 5(b)].

The correlation coefficient [16] is used to evaluate the similarity of frequency spectrum in order to determine whether the voltage variation on the healthy line is incurred by electromagnetic coupling or indeed a fault. The coefficient is defined in a crossed way as

$$C_1 = r(F(U_{pm}(\Delta T)), F(I_n(\Delta T))) \tag{7}$$

$$C_2 = r(F(U_{nm}(\Delta T)), F(I_p(\Delta T))) \tag{8}$$

where C_1 describes the coupling relation between the positive polarity of voltage and the negative polarity of current, andC_2 describes the coupling relation between the negative polarity of voltage and the positive polarity of current. These correlation coefficients are calculated after the fault with various time windows ($\Delta T = 0.0005$ and 0.002 s) for frequency-spectrum analysis, and the results are displayed in Fig. 6. The result shows that the voltage of the positive polarity and the current of negative polarity are highly correlated [C_1 remains large in Fig. 6(a)], disclosing that this voltage variation is induced by the transient current. On the other hand, the voltage of the negative polarity and the current of positive polarity are not coupled and thus uncorrelated [C_2 drops dramatically in Fig. 6(b)] since the voltage variation of the negative transmission line is incurred by the grounding fault. By comparing the sampling window of 0.0005 and 0.002 s, it can be observed that the shorter time window for frequency spectrum analysis

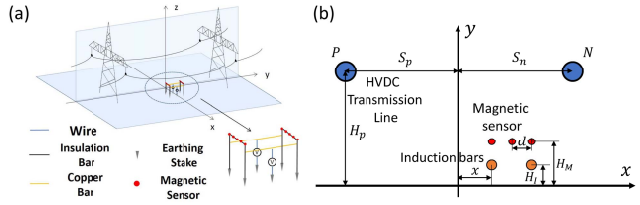

Fig. 7. Sensing platform for measuring line current and voltage at a point. (a) Spatial configuration of HVDC transmission line and sensing platform comprised magnetic sensors and induction bars. (b) Layout of HVDC transmission lines: $\boldsymbol{H_p} = 30$ m and $\boldsymbol{S_p} = \boldsymbol{S_n} = 2.5$ m. Induction bar: $\boldsymbol{x} = 1$ m and $\mathbf{H_I} = 0.5$ m. Magnetic sensor: $\boldsymbol{d} = 0.1$ m and $\boldsymbol{H_M} = 0.7$ m. And the platform was 10 km away from the rectifier side.

can provide a faster response time based on higher spectrum resolution. Therefore, the healthy line can be distinguished even with a large voltage variation, verifying the effectiveness of the proposed technique.

B. Implementation Based on Capacitive Coupling and Magnetic Field Sensing

The proposed identification technique was implemented on the same ±500 kV single-circuit HVDC system (Fig. 3), and the sensing platform was displayed in Fig. 7. The sensing components consist of magnetic sensors and induction bars [Fig. 7(a)], and their geometry is displayed in Fig. 7(b). The magnetic fields are measured by the magnetic sensors to reconstruct the phase current through a stochastic optimization program (SOP) as stated in [17] and [18], and the induced voltage of the induction bars are deployed to reconstruct the line voltage [19], [20]. The flowchart for attaining the line current and voltage at every time point can be found in Fig. 8(a). Currents (I) of HVDC transmission lines are reconstructed from the SOP [17] with the measured magnetic fields (B_m). The conductor spatial positions (P) can then be extracted. Voltages (V) are reconstructed from the voltage reconstruction program [21] with the measured induced voltage (V_m) of induction bars and the reconstructed conductor spatial positions (P). In this case, a phase-to-ground short-circuit fault was simulated at the positive polarity of HVDC transmission lines at 1 s. (The HVDC system, fault distance, and sensing point were the same as those in Fig. 3.) The comparison between the real and reconstructed current and voltage of HVDC transmission lines (the sampling frequency was 20 kHz) can be found in Fig. 8(b) and (c), and they closely match with each other. The correlation coefficients are calculated from the reconstructed voltages and currents with a 0.0005 s time window after the fault, and the result is displayed in Fig. 8(d). The voltage of negative polarity is highly correlated with the current of the positive polarity (C_2 remains large), revealing this voltage variation is induced by the transient current of the positive pole. As such, the voltage protection system should not take the negative polarity as fault even with a large voltage variation. Similarly, a phase-to-phase fault between positive and negative polarities was simulated. (The HVDC system, fault distance, and sensing point were the same as those in Fig. 3.) The correlation

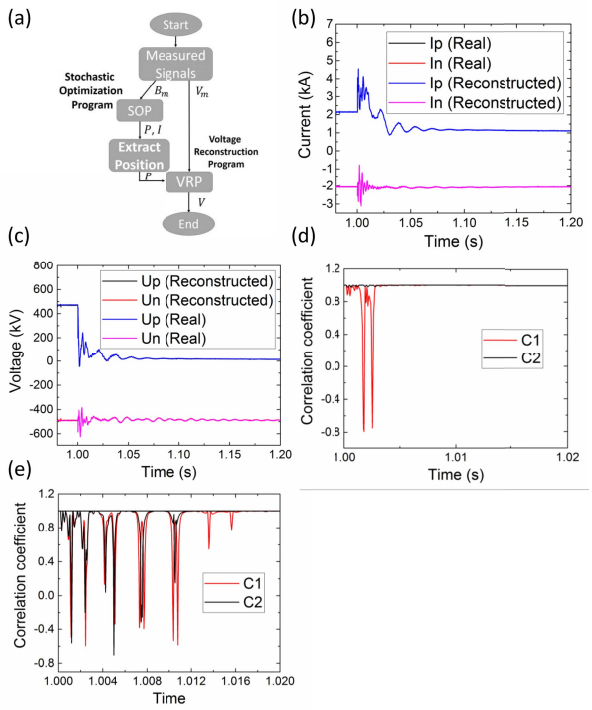

Fig. 8. Technique validation by simulation on a ±500 kV HVDC transmission system connecting two ac systems. (a) Flowchart for reconstructing voltage and current. (b) Real and reconstructed current of positive pole (I_p) and negative pole (I_n). (c) Real and reconstructed current of positive pole (U_p) and negative pole (U_n). (d) Correlation coefficients for the phase-to-ground short circuit fault at the positive polarity. (e) Correlation coefficients for the phase-to-phase fault.

coefficients were calculated as in Fig. 8(e), and the results show no coupling between the voltage of positive polarity and current of negative polarity or between the voltage of negative polarity and current of positive polarity. This indicates there did not exist electromagnetic coupling and it was a phase-to-phase fault. All these results verified the effectiveness of the technique.

IV. Conclusion

The similarity degree of frequency spectrum between the voltage of a line and current of another can be used to identify whether the voltage variation is incurred by electromagnetic coupling or fault under transient duration. The correlation coefficient was proposed to evaluate the similarity of frequency spectrum and this technique was validated by simulation on a ±500 kV HVDC transmission system. A voltage- and current-sensing platform comprised magnetic sensors and induction bars was also integrated into the simulation model to implement this technique. Its effectiveness was validated for a phase-to-ground short-circuit fault and phase-to-phase fault. This identification technique can enhance the reliability of HVDC system by accurately determining whether the voltage variation is due to electromagnetic coupling or indeed fault and thus avoiding the unnecessary outages due to accidental shutdown of healthy lines. It will be greatly conducive to the interconnection of power centers with the use of HVDC system for increased power transmission capacity.

In the future work, we will verify its effectiveness in an HVDC system under the real electromagnetic environment [22]–[24].

ACKNOWLEDGMENT

This work was supported in part by the Seed Funding Program for Basic Research, Seed Funding Program for Applied Research, and Small Project Funding Program from The University of Hong Kong, Hong Kong, in part by ITF Tier 3 Funding under Grant ITS-104/13 and Grant ITS-214/14, and in part by University Grants Committee of HK under Grant AoE/P-04/08.

REFERENCES

[1] N. Flourentzou, V. G. Agelidis, and G. D. Demetriades, "VSC-based HVDC power transmission systems: An overview," *IEEE Trans. Power Electron.*, vol. 24, no. 3, pp. 592–602, Mar. 2009.

[2] B. Zhang, X. Cui, R. Zeng, and J. He, "Calculation of DC current distribution in AC power system near HVDC system by using moment method coupled to circuit equations," *IEEE Trans. Magn.*, vol. 42, no. 4, pp. 703–706, Apr. 2006.

[3] T. Lu, H. Feng, Z. Zhao, and X. Cui, "Analysis of the electric field and ion current density under ultra high-voltage direct-current transmission lines based on finite element method," *IEEE Trans. Magn.*, vol. 43, no. 4, pp. 1221–1224, Apr. 2007.

[4] A. E. Hammad, "Stability and control of HVDC and AC transmissions in parallel," *IEEE Trans. Power Del.*, vol. 14, no. 4, pp. 1545–1554, Oct. 1999.

[5] M. Abdel-Salam, *High-Voltage Engineering: Theory and Practice, Revised and Expanded*, 2nd ed. Boca Raton, FL, USA: CRC Press, 2000.

[6] M. G. Adamiak *et al.*, "Wide area protection—Technology and infrastructures," *IEEE Trans. Power Del.*, vol. 21, no. 2, pp. 601–609, Apr. 2006.

[7] D. Naidoo and N. M. Ijumba, "A protection system for long HVDC transmission lines," in *Proc. Power Eng. Soc. Inaugural Conf. Expo. Africa*, Jul. 2005, pp. 150–155.

[8] H. Guo, W. Qingfan, and J. Huang, "Study on the influence of electromagnetic coupling of UHVDC power transmission lines on the voltage derivative protection," *Power Syst. Protection Control*, vol. 43, no. 18, pp. 114–119, 2015.

[9] Y. Liang, G. Wang, H. Li, and J. Wu, "Fault line selection for double-circuit HVDC transmission lines based on electric potential coefficients," *Auto Elec. Power Syst.*, vol. 40, no. 3, pp. 97–102, 2016.

[10] C. M. Franck, "HVDC circuit breakers: A review identifying future research needs," *IEEE Trans. Power Del.*, vol. 26, no. 2, pp. 998–1007, Apr. 2011.

[11] O. Mawardi, A. Gattozzi, and A. Ferendeci, "High voltage superconducting switch for power application," *IEEE Trans. Magn.*, vol. MAG-19, no. 3, pp. 1067–1070, May 1983.

[12] P. Liu, R. Che, Y. Xu, and H. Zhang, "Detailed modeling and simulation of +500 kV HVDC transmission system using PSCAD/EMTDC," in *Proc. IEEE PES Asia-Pacific Power Energy Eng. Conf. (APPEEC)*, Nov. 2015, pp. 1–3.

[13] R. N. Bracewell, *The Fourier Transform and Its Applications*. New York, NY, USA: McGraw-Hill, 1986.

[14] R. Taylor, "Interpretation of the correlation coefficient: A basic review," *J. Diagnostic Med. Sonogr.*, vol. 6, pp. 35–39, Jan. 1990.

[15] G. Mian, "An algorithm for a real time measurement of nonlinear transition shift by a time domain correlation analysis," *IEEE Trans. Magn.*, vol. 31, no. 1, pp. 816–819, Jan. 1995.

[16] J. L. Rodgers and W. A. Nicewander, "Thirteen ways to look at the correlation coefficient," *Amer. Statist.*, vol. 42, no. 1, pp. 59–66, 1988.

[17] K. Zhu, W. Han, W. K. Lee, and P. W. T. Pong, "On-site non-invasive current monitoring of multi-core underground power cables with a magnetic-field sensing platform at a substation," *IEEE Sensors J.*, vol. 17, no. 6, pp. 1837–1848, Mar. 2017.

[18] X. Sun, Q. Huang, Y. Hou, L. Jiang, and P. W. T. Pong, "Noncontact operation-state monitoring technology based on magnetic-field sensing for overhead high-voltage transmission lines," *IEEE Trans. Power Del.*, vol. 28, no. 4, pp. 2145–2153, Oct. 2013.

[19] K. Zhu, W. K. Lee, and P. W. T. Pong, "Non-contact electric-coupling-based and magnetic-field-sensing-assisted technique for monitoring voltage of overhead power transmission lines," in *Proc. IEEE Conf. Sensors.*, Nov. 2015, pp. 1–4.

[20] K. Zhu and P. W. T. Pong. *Non-Contact Electric-Coupling-Based and Magnetic-Field-Sensing-Assisted Sensing Technique for Monitoring Voltage of HVDC Transmission Lines*. Accessed: Jan. 29, 2018. [Online]. Available: https://www.researchgate.net/profile/Ke_Zhu21/publications

[21] K. Zhu, W. K. Lee, and P. W. T. Pong, "Non-contact capacitive-coupling-based and magnetic-field-sensing-assisted technique for monitoring voltage of overhead power transmission lines," *IEEE Sensors J.*, vol. 17, no. 4, pp. 1069–1083, Feb. 2017.

[22] C. W. Trowbridge, "Electromagnetic computing: The way ahead?" *IEEE Trans. Magn.*, vol. MAG-24, no. 1, pp. 13–18, Jan. 1988.

[23] M. Sibanda, R. van Zyl, and N. Parus. *Electromagnetic Environment Around HVDC Transmission Lines*. Accessed: Jan. 29, 2018. [Online]. Available: http://www.ee.co.za/article/icue-235-11-overview-of-the-electromagnetic-environment-in-the-vicinity-of-hvdc-transmission-lines.html

[24] P. S. Maruvada, "Electric field and ion current environment of HVDC transmission lines: Comparison of calculations and measurements," *IEEE Trans. Power Del.*, vol. 27, no. 1, pp. 401–410, Jan. 2012.